



Published in final edited form as:

Langmuir. 2013 February 26; 29(8): 2465–2470. doi:10.1021/la3037549.

Ligand-Mediated Self-Assembly of Hybrid Plasmonic and Superparamagnetic Nanostructures

Ryan L. Truby, Stanislav Y. Emelianov*, and Kimberly A. Homan

Department of Biomedical Engineering, The University of Texas at Austin, 1 University Station C0800, Austin, Texas, 78712, USA

Abstract

Hybrid nanostructures with unique optical and magnetic properties have attracted considerable interest as effective mediators for medical imaging and therapy. An aqueous-based, self-assembly approach to synthesizing hybrid plasmonic-superparamagnetic nanostructures is presented. The building blocks of the hybrid nanostructure include plasmonic gold nanorods (AuNRs) and superparamagnetic iron oxide nanoparticles (SPIONs). The AuNRs were functionalized via carboxyl-bearing surface ligands, while the SPIONs were kept “bare” after synthesis via a surfactant-free, thermal decomposition reaction in triethylene glycol. Hybrid SPION-studded AuNR nanostructures were produced upon simple mixing of the components due to chemisorption of the AuNRs’ free carboxyl groups to the SPIONs’ surfaces. The reported synthesis strategy is modular in nature and can be expanded to build hybrid nanostructures with a multitude of other plasmonic nanoparticles. With tunable near-infrared absorption peaks and a sufficient number of bound SPIONs, the self-assembled hybrid nanostructures are suitable for biomedical imaging and therapy applications.

Keywords

Hybrid nanostructures; self-assembly; gold nanoparticles; iron oxide; silica; plasmonic nanoparticles; superparamagnetic nanoparticles

INTRODUCTION

Plasmonic and superparamagnetic nanostructures have played extensive roles in emerging biomedical technologies. Exogenous nanoparticle contrast agents possessing optical extinction cross-sections in the near-infrared (NIR) spectrum have been crucial to the success of photothermal therapies,¹ molecular photoacoustic imaging,² and novel optical detection strategies.³ Similarly, superparamagnetic iron oxide nanoparticles (SPIONs) have been employed as agents for magnetic resonance imaging (MRI) contrast,⁴ contrast for magneto-motive-based imaging modalities,^{5,6} and novel thermal therapies.⁷ In turn, the endowment of simultaneous plasmonic and superparamagnetic properties on a single hybrid nanostructure opens myriad opportunities for improving the functionality and efficacy of novel therapeutic,⁸ molecular imaging,^{9–11} and biosensing¹² techniques.

*Corresponding Author: emelian@mail.utexas.edu.

Author Contributions

The manuscript was written through contributions of all authors. All authors have given approval to the final version of the manuscript.

Supporting Information. Detailed experimental methods, additional UV-Vis data, TEM images from control and silica-coating studies. This material is available free of charge via the Internet at <http://pubs.acs.org>.

Reports in the last several years have detailed the synthesis of an array of hybrid plasmonic-superparamagnetic nanoparticles (HPSNPs), including HPSNPs with core-shell,^{13–17} dumbbell,¹⁸ and cluster-like¹⁹ morphologies that are composed of both plasmonic and superparamagnetic materials. HPSNPs have also been fabricated by “bottom-up” approaches that join individually synthesized superparamagnetic and plasmonic nanostructures together through conjugation chemistry,^{20–22} self-assembly,^{23–25} and liposomal packing.²⁶ Ideally, HPSNPs for biomedical applications should i) exhibit plasmon resonances in the NIR optical window that yield NIR absorption and scattering cross-sections necessary for optimal optical excitation of the HPSNPs in vivo, ii) possess a high magnetic volume fraction, and iii) be functionalized with biocompatible coatings that limit immune system recognition of nanostructures in vivo and allow for extravasation into pathologies with leaky vascular networks via the enhanced permeability and retention effect.²⁷ As interest in HPSNPs continues to rise, it is becoming evermore imperative that the materials community produce hybrid nanostructures with tailorable magnetic and NIR optical properties via facile, biofriendly synthesis reactions.

Herein, we report a simple, aqueous-based, self-assembly approach to the synthesis of HPSNPs that eliminates the need for conjugation chemistry, organic surfactants with aliphatic or hydrophobic tail groups, and/or hydrocarbon solvents (all of which have been techniques or reagents employed in previously reported HPSNP syntheses^{10,13–15,17,18,22,23,25}). First, by exploiting SPIONs’ affinity for carboxylic acid (–COOH) moieties,^{28,29} SPION-studded gold nanorods (SPION-AuNRs) are self-assembled through the mixing of “bare” SPIONs with gold nanorods (AuNRs) whose surfaces are functionalized with bifunctional poly(ethylene glycol) (PEG) chains with terminal –COOH groups. The “bare” SPIONs are stabilized by a coating of triethylene glycol (TREG) that is easily displaced by the chemisorption of –COOH to the SPIONs’ surfaces. Multiple “bare” SPIONs are capable of chemisorbing to or “studding” the surfaces of the –COOH-functionalized AuNRs (COOH-AuNRs),^{28,29} ensuring that the hybrid nanostructure maintains a large magnetic volume fraction and, consequently, a sufficiently high saturation magnetization. Second, we demonstrate the modular nature and optical tunability of our self-assembly synthesis strategy by additionally synthesizing SPION-studded gold nanoplates (SPION-AuNPs) that absorb NIR light of longer wavelengths. This feature allows the presented synthesis scheme to be easily adapted for constructing hybrid nanostructures with other plasmonic nanoparticles. Finally, due to the stable nature of the chemisorption interactions between the SPIONs and plasmonic nanoparticles in our HPSNPs, our self-assembly approach to synthesizing HPSNPs represents a facile, non-toxic approach to synthesizing HPSNPs appropriate for use in multimodal, biomedical technologies.

EXPERIMENTAL METHODS

The synthesis strategy for the SPION-AuNRs is illustrated in Scheme 1. First, cetyltrimethylammonium bromide (CTAB)-coated AuNRs (CTAB-AuNRs) were obtained with a synthesis reaction adapted from a previously reported seed-mediated protocol.³⁰ It has been demonstrated that the physisorbed CTAB surfactant layer coating the AuNRs is cytotoxic but can be replaced by ligands bearing thiol (–SH) groups that form thiolate bonds with gold atoms on the nanorod surface.³¹ Therefore, a solution of CTAB-AuNRs with an optical density (OD) between 13 and 15 was mixed with an equal volume of a 0.2 mM solution of heterobifunctional –COOH and –SH terminated poly(ethylene glycol) (PEG) chains (COOH-PEG-SH) with a molecular weight of 5000 Da. Replacement of the CTAB surface layer not only improved the biocompatibility of the AuNRs, but also left the AuNRs functionalized with free –COOH groups necessary for later forming the hybrid nanostructure. In short, the formation of gold-thiolate bonds between the COOH-PEG-SH

and CTAB-AuNR resulted in the displacement of CTAB surface layers and the ultimate PEGylation and –COOH-functionalization of the AuNRs' surfaces.

Next, the “bare,” TREG-stabilized superparamagnetic iron oxide nanoparticles (TREG-SPIONs) were synthesized via a thermal decomposition reaction of 1 g iron (III) acetylacetonate ($\text{Fe}(\text{acac})_3$) in 20 mL TREG without a surfactant present and under an inert argon atmosphere.³² Thermal decomposition reactions serve as ideal synthesis methods for SPIONs on account of their ability to yield highly monodispersed SPION products of nearly spherical species.²⁹ However, such reactions require the use of solvents with boiling points well over the 180°C, the melting point of $\text{Fe}(\text{acac})_3$. Consequently, high molecular weight, toxic organic solvents are commonly employed in such syntheses.³³ We chose TREG as the solvent for SPION synthesis since it eliminated the need for toxic organic solvents during synthesis, is a suitable high boiling point solvent, and serves as a reducing agent necessary to induce decomposition of $\text{Fe}(\text{acac})_3$ into free ferric and ferrous ions.³² Furthermore, surfactants such as oleic acid are commonly used during SPION synthesis since they chemisorb to the SPION surface and help control the nanoparticles' growth, size, and morphology.³³ A surfactant-free method was chosen here since strongly adsorbed surfactants substantially hinder the surface reactivity of SPIONs. TREG serves as a weak stabilizing agent that can later be easily displaced by surfactants, polymers, and other ligands expressing –COOH groups, which have a strong, well-characterized affinity for ferrous ions.^{28,29} The TREG-SPIONs are therefore referred to as “bare” on account of their surfaces' high, unhindered reactivity with –COOH groups.

Finally, for SPION-AuNR synthesis, 100 μL of TREG-SPION solution was cleaned by several centrifugation steps and washings with 1.5 mL of 1:1 ethanol and ethyl acetate mixture, dried in nitrogen, and suspended in 2 mL of an aqueous hydrochloric acid (HCl) solution (pH = 3.5). To this solution, 2 mL of COOH-AuNR solution was added, and the reaction mixture was sonicated for 5 minutes and allowed to react for 1 hr while vortexing at 500 rpm. Upon mixing, the carboxyl-terminated PEG chains provided by the COOH-AuNRs served as chemisorption sites for the TREG-SPIONs. The ratio of TREG-SPIONs to COOH-AuNRs in the self-assembly reaction was sufficiently large to permit the TREG-SPIONs to overwhelm the free COOH-AuNR surface area. If the TREG-SPION to COOH-AuNR ratio was too low, obvious and nearly immediate aggregation resulted from the chemisorption of multiple COOH-AuNRs to the same TREG-SPIONs (see Figure S1 in Supporting Information). SPION-AuNRs were separated from excess, unbound SPIONs by light centrifugation for 30 min at 1,500 g. The collected SPION-AuNR pellet was resuspended in 2 mL of deionized ultrafiltered (18.2 M Ω -cm.) (DIUF) water. The morphologies of the COOH-AuNRs, TREG-SPION, and SPION-AuNRs were analyzed with transmission electron microscopy (TEM, Hitachi S5500 Scanning/Transmission Electron Microscope). Superconducting quantum interference device (SQUID) magnetometry (MPMS SQUID VSM, Quantum Design) was used to determine the superparamagnetic response of the TREG-SPIONs, and extinction spectra of plasmonic and hybrid plasmonic-superparamagnetic nanostructures were obtained via UV-Vis spectrophotometry (DU Series 600 Spectrophotometer, Beckman Coulter). Zeta potential measurements were obtained with a Delsa Nano (Beckman Coulter).

RESULTS AND DISCUSSION

Representative TEM images of the COOH-AuNRs and TREG-SPIONs are shown in Figure 1A and Figure 1B, respectively. The TREG-SPIONs were roughly spherical in shape and had a mean diameter of 7.5 ± 1.2 nm, which was calculated with ImageJ software from a sample population of 475 nanoparticles. As seen in Figure 1C, the TREG-SPIONs successfully chemisorbed to the COOH-AuNRs' surfaces, yielding the desired hybrid

SPION-AuNR nanostructures. As a control study, the same TREG-SPIONs were reacted with AuNRs that had been PEGylated with methoxy-poly(ethylene glycol)-thiol (mPEG-SH). Without free –COOH groups at their surfaces, it was not expected that the SPION-AuNRs would form upon mixing of these mPEG-SH-coated AuNRs (mPEG-AuNRs) and TREG-SPIONs. As evident from Figure 1D, TEM confirmed that without free –COOH groups present, SPION-AuNRs do not form: only a mixture of mPEG-AuNRs and TREG-SPIONs is present.

The TREG-SPIONs exhibited a saturation magnetization of 58 emu per g of nanoparticles according to SQUID magnetometry (see Figure 2A). As seen in the UV-Vis spectrophotometry data of Figure 2B, the CTAB-AuNRs possessed plasmon resonances within the NIR range, and PEGylation of the CTAB-AuNRs with COOH-PEG-SH did not significantly alter the NIR optical properties of the AuNRs. PEGylation resulted in a blue-shift of the extinction peak between 20 and 40 nm (see the red and blue spectra in Figure 2B).

The extinction maximum observed for the SPION-AuNRs collected by centrifugation consistently exhibited a red-shift of approximately 25 nm with respect to the COOH-AuNRs (see the blue and light purple spectra in Figure 2B). Other studies have reported red-shifts of approximately 20 to 35 nm in extinction maximum upon studding plasmonic noble metal nanoparticles with similarly-sized iron oxide nanoparticles.^{20,24} Thus, in conjunction with the TEM data presented in Figure 1, the 25-nm red-shift observed for the resuspended nanoparticle pellet obtained from the reaction of COOH-AuNRs and TREG-SPIONs indicates the presence of SPION-AuNRs. UV-Vis extinction spectra were also obtained from the control study with mPEG-SH and are provided in Figure S2 in the Supporting Information. The centrifuged product of the control study, which was expected to not contain SPION-AuNRs, exhibited a ~10-nm red-shift in extinction maximum with respect to the extinction peak for mPEG-AuNRs. We attribute this minor red-shift in extinction peak to non-specific interaction between the mPEG-AuNRs and remaining TREG-SPIONs in solution. Lastly, upon their collection by microcentrifugation and resuspension in nanopure water, a slight broadening of the extinction spectrum was observed. This broadening is likely the result of minimal nanoscale aggregation between SPION-AuNRs as they are forced closer towards other SPION-AuNRs during the centrifugation step (see Figure S4 in the Supporting Information).

The colloidal stability of the cleaned TREG-SPIONs was essential to the successful synthesis of the hybrid SPION-AuNRs. In the course of our experiments, we found that the cleaned TREG-SPIONs were not highly dispersible in water. However, by suspending them in an aqueous HCl or NaOH solution, the TREG-SPIONs' colloidal stability drastically improved. Acidic, basic, and DIUF water suspensions of TREG-SPIONs were reacted with aqueous suspensions of COOH-AuNRs, but the desired SPION-AuNRs only self-assembled when TREG-SPIONs in aqueous HCl solutions were used (see Figure S3 in Supporting Information).

Studies have shown that “bare” SPIONs synthesized by co-precipitation reactions become positively charged in acidic solutions, suggesting that “bare” TREG-SPIONs also become positively charged in acidic solutions.^{28,29} This was confirmed by zeta potential measurements. In aqueous HCl solution (pH = 3), TREG-SPIONs had zeta potentials of approximately 37 mV. Resuspended in the same HCl solution, COOH-AuNRs possessed zeta potentials of approximately –68 mV, revealing that there are free –COOH groups on the surfaces of the COOH-AuNRs that remain deprotonated during the self-assembly synthesis reaction. Thus, the self-assembly of SPION-AuNRs was facilitated by the HCl solution by

creating an electrostatic attraction between positively charged TREG-SPIONs and negatively charged COOH-AuNRs.

Our ligand-mediated, self-assembly approach is also modular in nature. Any plasmonic nanoparticle that is capable of forming thiolate bonds with COOH-PEG-SH and remaining stable in HCl solutions can be substituted for the COOH-AuNRs. Therefore, our method enables the synthesis of HPSNPs possessing practically limitless options of extinction spectra. The modular feature of the presented HPSNP self-assembly-based synthesis was demonstrated by mixing TREG-SPIONs with gold nanoplates (AuNPs) that had been PEGylated with COOH-PEG-SH (COOH-AuNPs, see Figure 3A). Figure 3B shows a TEM image of COOH-AuNPs with multiple TREG-SPIONs chemisorbed to their surfaces, forming SPION-studded AuNPs (SPION-AuNPs). The SPION-AuNPs maintained similar plasmonic properties to the COOH-AuNPs according to the extinction spectra shown in Figure 3C. By synthesizing the SPION-AuNPs, we have demonstrated the modular feature of our HPSNP synthesis method.

For many multimodal medical imaging applications, it is desirable for the plasmonic and superparamagnetic components of an HPSNP to remain bound *in vivo* if the hybrid nanostructure is employed as a dual imaging contrast agent. Under intense laser irradiation or under exposure to extreme temperatures, the chemisorption interactions between the COOH-AuNR and TREG-SPIONs or the gold-thiolate bonds anchoring the COOH-PEG-SH to the AuNRs could be insufficiently strong to keep the SPION-AuNRs intact.³⁴ We have silica-coated the SPION-AuNRs, in a preliminary effort, using a modified Stöber method for silica-coating AuNRs³⁴ to demonstrate the feasibility of creating a more stable HPSNP (see Supporting Information) that will remain intact under intense thermal conditions. Additionally, this silica-coating study offers additional support to the claim that the TREG-SPIONs do in fact chemisorb to the COOH-AuNRs: as seen in Figure 4; the silica-coating reaction coats the SPION-AuNRs, rather than dissociating them and producing silica-coated COOH-AuNRs and silica-coated TREG-SPIONs.

CONCLUSION

SPION-AuNRs were synthesized by the mixing of strategically functionalized plasmonic AuNR and superparamagnetic TREG-SPION components and characterized through UV-Vis spectrophotometry and TEM. Given their small size, NIR optical properties, and high magnetic volume fraction, the SPION-AuNRs can serve as HPSNPs for biomedical applications. Our –COOH ligand-mediated self-assembly approach allows for the optical tunability of the SPION-AuNRs and presents a more facile approach for HPSNP synthesis that does not require bioconjugation steps or toxic compounds. As demonstrated by the synthesis of SPION-AuNPs, the presented HPSNP synthesis method can be extended for any plasmonic nanoparticle that readily forms metal-thiolate bonds with COOH-PEG-SH. Thus, the HPSNPs produced from the proposed ligand-mediated, self-assembly synthesis method are promising for employment in a host of multimodal biomedical imaging and therapeutic applications requiring superparamagnetic and plasmonically active agents.

Supplementary Material

Refer to Web version on PubMed Central for supplementary material.

Acknowledgments

Funding Sources

We acknowledge and appreciate the research support R. L. Truby received from the Junior Fellows Program and an Undergraduate Research Fellowship from The Office of the Vice President for Research at The University of Texas at Austin. We recognize the National Science Foundation (grant No. 0821312) for funding the Hitachi S-5500 STEM used in this work as well as support from the National Institutes of Health (grants CA 149740 and EB 008821).

The authors would like to thank Dr. Yun-Sheng Chen, Pratixa Joshi, Geoffrey Luke, Dr. Mohammad Mehrmohammadi, Dr. Min Qu, and Dr. Katheryne Wilson at The University of Texas at Austin for their insightful discussions into the characterization, potential biomedical applications, and silica coating of the hybrid plasmonic-superparamagnetic nanoparticles presented. The authors also acknowledge Dr. Mohammad Mehrmohammadi and Dr. Jianshi Zhou of The University of Texas at Austin for their assistance in obtaining the SQUID data. R. L. Truby personally thanks Erika Vreeland and Dr. Dale Huber of the Center for Integrated Nanotechnologies at Sandia National Laboratories for their indispensable knowledge into the synthesis and characterization of superparamagnetic nanoparticles.

ABBREVIATIONS

NIR	near-infrared
SPION	superparamagnetic iron oxide nanoparticle
HPSNP	hybrid plasmonic-superparamagnetic nanoparticle
SPION-AuNR	superparamagnetic iron oxide nanoparticle-studded gold nanorod
-COOH	carboxylic acid
AuNR	gold nanorod
TREG	triethylene glycol
COOH-AuNRs	carboxylic acid-functionalized gold nanorods
CTAB	cetyltrimethylammonium bromide
CTAB-AuNRs	cetyltrimethylammonium bromide-coated gold nanorods
-SH	thiol
OD	optical density
PEG	polyethylene glycol
COOH-PEG-SH	heterobifunctional carboxylic acid and thiol terminated polyethylene glycol
TREG-SPIONS	triethylene glycol-stabilized superparamagnetic iron oxide nanoparticles
Fe(acac)₃	iron (III) acetylacetonate
HCl	hydrochloric acid
SQUID	superconducting quantum interference device
TEM	transmission electron microscopy
mPEG-SH	methoxy-poly(ethylene glycol)-thiol
mPEG-AuNRs	mPEG-SH coated AuNRs
PBS	phosphate buffered saline
NaOH	sodium hydroxide
AuNP	gold nanoplate
COOH-AuNP	carboxylic acid-functionalized gold nanoplates

SPION-AuNP

superparamagnetic iron oxide nanoparticle-studded gold nanoplate

References

- Huang X, El-Sayed IH, Qian W, El-Sayed MA. Cancer Cell Imaging and Photothermal Therapy in the Near-Infrared Region by Using Gold Nanorods. *J Am Chem Soc.* 2006; 128:2115–2120. [PubMed: 16464114]
- Luke G, Yeager D, Emelianov S. Biomedical Applications of Photoacoustic Imaging with Exogenous Contrast Agents. *Ann Biomed Eng.* 2012; 40:422–437. [PubMed: 22048668]
- Xu L, Kuang H, Xu C, Ma W, Wang L, Kotov NA. Regiospecific Plasmonic Assemblies for in Situ Raman Spectroscopy in Live Cells. *J Am Chem Soc.* 2012; 134:1699–1709. [PubMed: 22192084]
- Jun Y, Lee JH, Cheon J. Chemical Design of Nanoparticle Probes for High-Performance Magnetic Resonance Imaging. *Angew Chem Int Edit.* 2008; 47:5122–5135.
- John R, Boppart SA. Magnetomotive Molecular Nanoprobes. *Curr Med Res Opin.* 2011; 18:2103–2114.
- Mehrmohammadi M, Oh J, Mallidi S, Emelianov SY. Pulsed Magneto-motive Ultrasound Imaging Using Ultrasmall Magnetic Nanoprobes. *Mol Imaging.* 2011; 10:102–110. [PubMed: 21439255]
- Lee JH, Jang J-t, Choi J-s, Moon SH, Noh S-h, Kim J-w, Kim JG, Kim IS, Park KI, Cheon J. Exchange-coupled magnetic nanoparticles for efficient heat induction. *Nature Nanotech.* 2011; 6:418–422.
- Riedinger A, Leal MP, Deka SR, George C, Franchini IR, Falqui A, Cingolani R, Pellegrino T. ‘Nanohybrids’ Based on pH-Responsive Hydrogels and Inorganic Nanoparticles for Drug Delivery and Sensor Applications. *Nano Lett.* 2011; 11:3136–3141. [PubMed: 21692456]
- Aaron JS, Oh J, Larson TA, Kumar S, Milner TE, Sokolov KV. Increased optical contrast in imaging of epidermal growth factor receptor using magnetically actuated hybrid gold/iron oxide nanoparticles. *Opt Express.* 2006; 14:12930–12943. [PubMed: 19532186]
- Wei Q, Song HM, Leonov AP, Hale JA, Oh D, Ong QK, Ritchie K, Wei A. Gyromagnetic Imaging: Dynamic Optical Contrast Using Gold Nanostars with Magnetic Cores. *J Am Chem Soc.* 2009; 131:9728–9734. [PubMed: 19435348]
- John R, Rezaeipoor R, Adie SG, Chaney EJ, Oldenburg AL, Marjanovic M, Haldar JP, Sutton BP, Boppart SA. In vivo magnetomotive optical molecular imaging using targeted magnetic nanoprobes. *PNAS.* 2010; 107:8085–8090. [PubMed: 20404194]
- Qu M, Mehrmohammadi M, Emelianov S. Detection of Nanoparticle Endocytosis Using Magneto-Photoacoustic Imaging. *Small.* 2011; 7:2858–2862. [PubMed: 21910248]
- Wang L, Luo J, Fan Q, Suzuki M, Suzuki IS, Engelhard MH, Lin Y, Kim N, Wang JQ, Zhong CJ. Monodispersed Core-Shell Fe₃O₄@Au Nanoparticles. *J Phys Chem B.* 2005; 109:21593–21601. [PubMed: 16853803]
- Jin Y, Jia C, Huang S-W, O’Donnell M, Gao X. Multifunctional nanoparticles as coupled contrast agents. *Nat Commun.* 2010; 110.1038/ncomms1042
- Kumagai M, Sarma TK, Cabral H, Kaida S, Sekino M, Herlambang N, Osada K, Kano MR, Nishiyama N, Kataoka K. Enhanced in vivo Magnetic Resonance Imaging of Tumors by PEGylated Iron-Oxide-Gold Core-Shell Nanoparticles with Prolonged Blood Circulation Properties. *Macromol Rapid Commun.* 2010; 31:1521–1528. [PubMed: 21567561]
- Bhana S, Rai BK, Mishra SR, Wang Y, Huang X. Synthesis and properties of near infrared-absorbing magnetic-optical nanoprobes. *Nanoscale.* 2012; 4:4939–4942. [PubMed: 22806589]
- Xia W, Song HM, Wei Q, Wei A. Differential response of macrophages to core-shell Fe₃O₄@Au nanoparticles and nanostars. *Nanoscale.* 2012; 4:7143–7148. [PubMed: 23069807]
- Gu H, Yang Z, Gao J, Chang CK, Xu B. Heterodimers of Nanoparticles: Formation at a Liquid-Liquid Interface and Particle-Specific Surface Modification by Functional Molecules. *J Am Chem Soc.* 2004; 127:34–35. [PubMed: 15631435]
- Ma LL, Feldman MD, Tam JM, Paranjape AS, Cheruku KK, Larson TA, Tam JO, Ingram DR, Paramita V, Villard JW, Jenkins JT, Wang T, Clarke GD, Asmis R, Sokolov K, Chandrasekar B,

- Milner TE, Johnson KP. Small Multifunctional Nanoclusters (Nanoroses) for Targeted Cellular Imaging and Therapy. *ACS Nano*. 2009; 3:2686–2696. [PubMed: 19711944]
20. Wang C, Chen J, Talavage T, Irudayaraj J. Gold nanorod/Fe₃O₄ nanoparticle ‘nano-pearl-necklaces’ for simultaneous targeting, dual-mode imaging, and photothermal ablation of cancer cells. *Angew Chem Int Ed*. 2009; 48:2759–2763.
 21. Wang C, Irudayaraj J. Multifunctional Magnetic-Optical Nanoparticle Probes for Simultaneous Detection, Separation, and Thermal Ablation of Multiple Pathogens. *Small*. 2009; 6:283–289. [PubMed: 19943255]
 22. Basiruddin S, Maity AR, Saha A, Jana NR. Gold-Nanorod-Based Hybrid Cellular Probe with Multifunctional Properties. *J Phys Chem C*. 2011; 115:19612–19620.
 23. Wang M, Wang C, Young KL, Hao L, Medved M, Rajh T, Fry HC, Zhu L, Karczmar GS, Watson C, Jiang JS, Markovic NM, Stamenkovic VR. Cross-linked Heterogeneous Nanoparticles as Bifunctional Probe. *Chem Mater*. 2012; 24:2423–2425.
 24. Zhai Y, Han L, Wang P, Li G, Ren W, Liu L, Wang E, Dong S. Superparamagnetic plasmonic nanohybrids: shape-controlled synthesis, TEM-induced structure evolution, and efficient sunlight-driven inactivation of bacteria. *ACS Nano*. 2011; 5:8562–8570. [PubMed: 21951020]
 25. Tian J, Zheng F, Zhao H. Nanoparticles with Fe₃O₄-Nanoparticle Cores and Gold-Nanoparticle Coronae Prepared by Self-Assembly Approach. *J Phys Chem C*. 2011; 115:3304–3312.
 26. Qu M, Mallidi S, Mehrmohammadi M, Truby R, Homan K, Joshi P, Chen YS, Sokolov K, Emelianov S. Magneto-photo-acoustic imaging. *Biomed Opt Express*. 2011; 2:385–396. [PubMed: 21339883]
 27. Maeda H. The enhanced permeability and retention (EPR) effect in tumor vasculature: the key role of tumor-selective macromolecular drug targeting. *Adv Enzyme Regul*. 2001; 41:189–207. [PubMed: 11384745]
 28. Lu Z, Qin Y, Fang J, Sun J, Li J, Liu F, Yang W. Monodisperse magnetizable silica composite particles from heteroaggregate of carboxylic polystyrene latex and Fe₃O₄ nanoparticles. *Nanotechnology*. 2008.1088/0957–4484/19/05/055602
 29. Ravikumar C, Bandyopadhyaya R. Mechanistic Study on Magnetite Nanoparticle Formation by Thermal Decomposition and Coprecipitation Routes. *J Phys Chem C*. 2011; 115:1380–1387.
 30. Nikoobakht B, El-Sayed MA. Preparation and Growth Mechanism of Gold Nanorods (NRs) Using Seed-Mediated Growth Method. *Chem Mater*. 2003; 15:1957–1962.
 31. Pierrat S, Zins I, Breivogel A, Sönnichsen C. Self-Assembly of Small Gold Colloids with Functionalized Gold Nanorods. *Nano Lett*. 2006; 7:259–263. [PubMed: 17297987]
 32. Maity D, Kale SN, Kaul-Ghanekar R, Xue JM, Ding J. Studies of magnetite nanoparticles synthesized by thermal decomposition of iron (III) acetylacetonate in tri(ethylene glycol). *J Magn Mater*. 2009; 321:3093–3098.
 33. Laurent S, Forge D, Port M, Roch A, Robic C, Elst LV, Muller RN. Magnetic Iron Oxide Nanoparticles: Synthesis, Stabilization, Vectorization, Physicochemical Characterizations, and Biological Applications. *Chem Rev*. 2008; 108:2064–2110. [PubMed: 18543879]
 34. Chen YS, Frey W, Kim S, Homan K, Kruizinga P, Sokolov K, Emelianov S. Enhanced thermal stability of silica-coated gold nanorods for photoacoustic imaging and image-guided therapy. *Opt Express*. 2010; 18:8867–8878. [PubMed: 20588732]

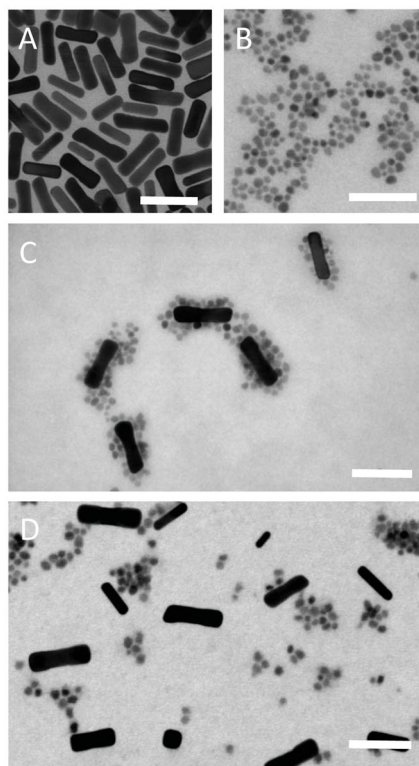


Figure 1. TEM images of (A) COOH-AuNRs, (B) TREG-SPIONs, (C) a reaction mixture of COOH-AuNRs and TREG-SPIONs showing SPION-AuNR formation, and (D) a reaction mixture of mPEG-AuNRs and TREG-SPIONs. The scale bar in each image represents 50 nm.

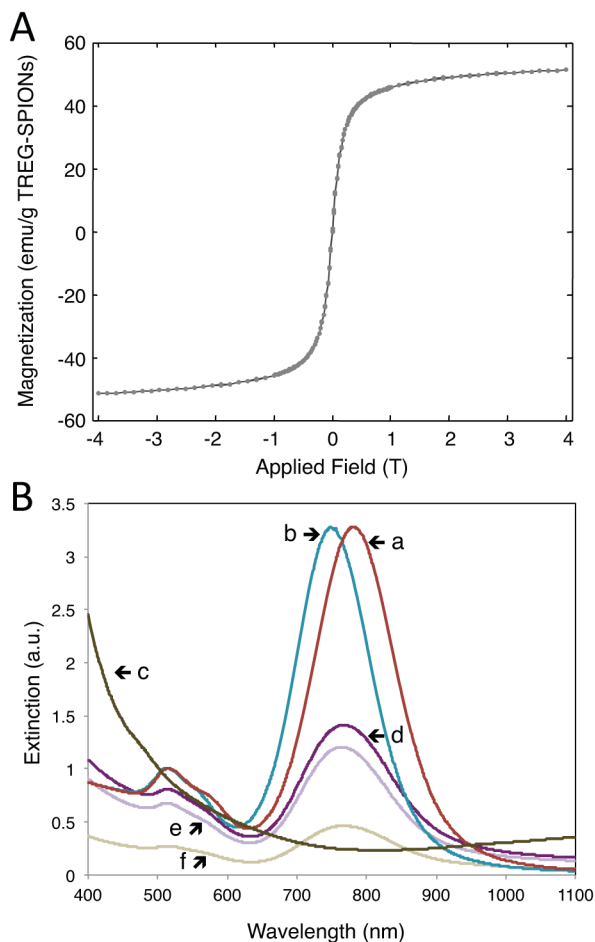


Figure 2.

(A) The magnetization response of TREG-SPIONs determined with SQUID magnetometry and (B) the UV-Vis extinction spectra for (line a) 4x diluted CTAB-AuNRs, (line b) 2x diluted COOH-AuNRs, (line c) 2x diluted cleaned TREG-SPIONs in pH = 3.5 solution, (line d) a 2x dilution of the reaction solution of TREG-SPIONs mixed with COOH-AuNRs, (line e) a 2x dilution of the SPION-AuNRs collected by centrifugation and resuspended in DIUF water, and (line f) a 1.3x dilution of the supernatant collected from the centrifuged pellet of SPION-AuNRs.

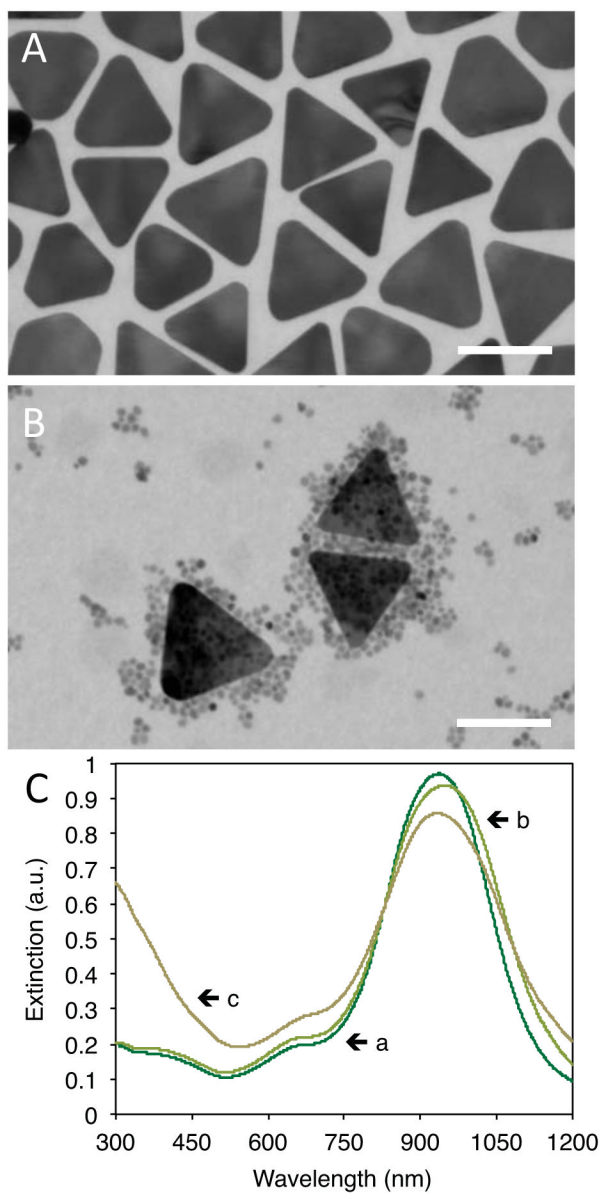


Figure 3. TEM images of (A) COOH-AuNPs and (B) SPION-AuNPs in a reaction mixture of TREG-SPIONs and COOH-AuNPs (scale bars represent 75 nm) and (C) UV-Vis extinction spectra for (line a) 30x diluted CTAB-AuNPs (OD = 30), (line b) 5.3x dilution of COOH-AuNPs, and (line c) the reaction mixture of TREG-SPIONs and COOH-AuNPs.

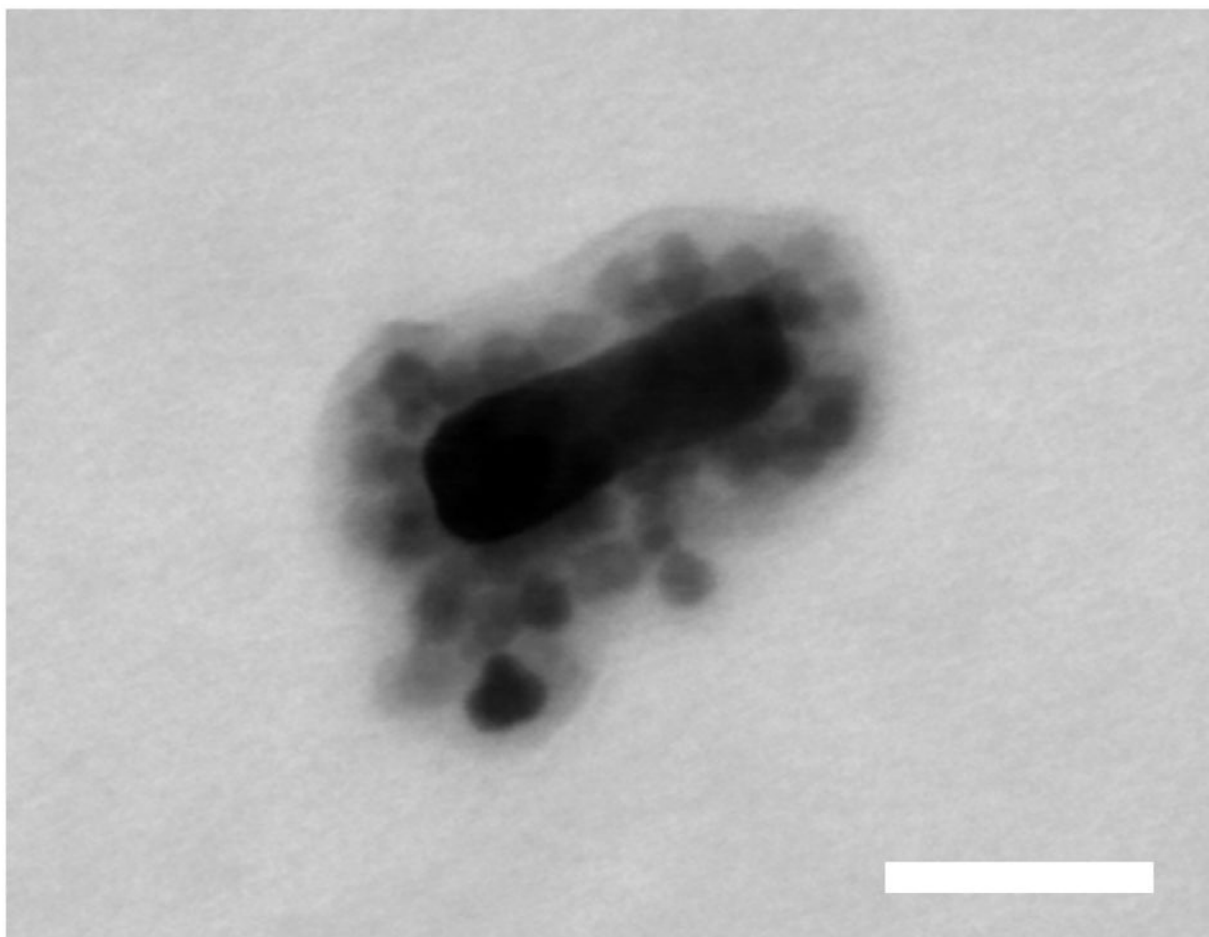
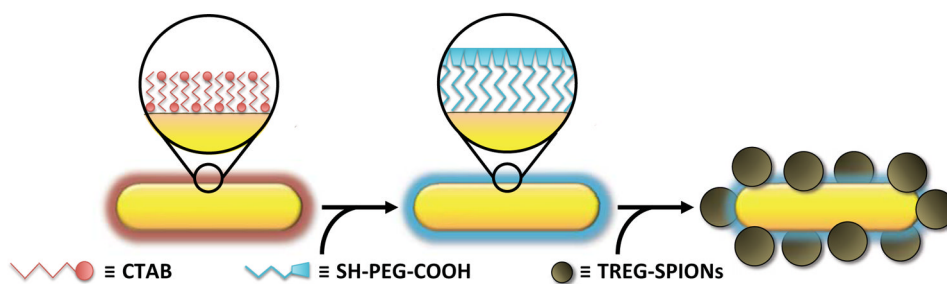


Figure 4.
(a) Representative TEM image of a single SPION-AuNR coated with a ~13 nm thick layer silica. Scale bar represents 30 nm.

**Scheme 1.**

Flow Diagram of the Self-Assembling Synthesis Method Depicting the Functionalization of CTAB-AuNRs with Free $-\text{COOH}$ Moieties and their Chemisorption to “Bare” SPIONs after Mixing the COOH -AuNRs and TREG-SPIONs